J Radioanal Nucl Chem (2015) 304:1077–1083
DOI 10.1007/s10967-015-3975-y

Production and separation of astatine isotopes in the ^{7}Li + ^{nat}Pb reaction

I. Nishinaka · A. Yokoyama · K. Washiyama · E. Maeda · S. Watanabe · K. Hashimoto · N. S. Ishioka · H. Makii · A. Toyoshima · N. Yamada · R. Amano

Received: 19 September 2014 / Published online: 14 February 2015

Abstract Production cross sections of astatine isotopes $^{207-211}$At in the 29–57 MeV ^{7}Li + ^{nat}Pb reaction have been measured by α- and γ-ray spectrometry. Excitation functions of production cross sections have been compared with a statistical calculation to study the reaction mechanism of the ^{7}Li + ^{nat}Pb reaction. Production reactions of $^{207-211}$At in the ^{7}Li + ^{nat}Pb have been derived. Considerably small experimental cross sections of ^{210}At and ^{209}At compared with the statistical calculation were clearly observed at incident energies higher than 44 MeV, indicating that the effects of breakup reaction play a role. A chemical separation of astatine from an irradiated lead target has been studied with a dry-distillation method. A complementary way to produce astatine isotopes has been developed.

Keywords Nuclear reaction · Production cross section · Excitation function · Astatine · Distillation

I. Nishinaka (✉) · H. Makii · A. Toyoshima
Advanced Science Research Center, Japan Atomic Energy Agency, Shirakata-Shirane 2-4, Tokai-mura, Naka-gun, Ibaraki 319-1195, Japan
e-mail: nishinaka.ichiro@jaea.go.jp

A. Yokoyama · E. Maeda · N. Yamada
Institute of Science and Engineering, Kanazawa University, Kakuma, Kanazawa, Ishikawa 920-1192, Japan

K. Washiyama · R. Amano
Institute of Medical, Pharmaceutical and Health Sciences, Kanazawa University, Kodatsuno 5-11-80, Kanazawa, Ishikawa 920-0942, Japan

S. Watanabe · K. Hashimoto · N. S. Ishioka
Quantum Beam Science Directorate, Japan Atomic Energy Agency, Watanuki 1233, Takasaki, Gunma 370-1292, Japan

Introduction

An α radioactive nuclide ^{211}At with a half-life ($T_{1/2}$) of 7.2 h is a prospective candidate for utilization in radioimmunotherapy. In a general way, ^{211}At is produced through bombardment of a bismuth target with 28 MeV helium ions in the ^{209}Bi(α,2n)^{211}At reaction because of the high specific activity required for therapeutic purpose [1–7]. However, the nuclear reactions using lithium ion beams, ^{6,7}Li + ^{nat}Pb and ^{6,7}Li + ^{209}Bi, provide the possible production routes of ^{211}At. Such complementary production in the lithium-induced reactions could make a contribution to the utilization of astatine isotopes, leading to the development of the utilization in radioimmunotherapy. Excitation functions have been extensively measured for the ^{6,7}Li + ^{209}Bi reactions to study the reaction mechanism involving complete fusion and breakup reaction of weakly bound nuclei, ^{6,7}Li [8–11]. For ^{7}Li + ^{nat}Pb, however, only a few reports on production of astatine isotopes $^{207-210}$At have been available [12, 13]. To produce and to use radioactive astatine isotopes, we have determined production cross sections of not only $^{207-210}$At but also ^{211}At in the ^{7}Li + ^{nat}Pb by α- and γ-ray spectrometry. Besides, a chemical separation has been studied with a dry-distillation method.

Experimental

Irradiation

Irradiation was carried out with ^{7}Li^{3+} beams of 50 and 60 MeV from the 20 MV tandem accelerator at JAEA-Tokai. Lead targets, aluminum backing and cover sheets were placed at a water-cooled Faraday cup as schematically

shown in Fig. 1. Lead (99.95 %, Goodfellow Corporation, Coraopolis, PA, USA) targets with thickness of 0.78–1.47 mg/cm^2 were prepared by vacuum evaporation onto a backing sheet of 5.4 mg/cm^2 aluminum (Toyo Aluminium K. K., Osaka, Japan). Each target was sandwiched between the backing and a cover sheet of 5.4 mg/cm^2 aluminum. The thickness of aluminum is enough to stop not only recoil nuclides but also fission fragments. Beam current was controlled to be approximately 80–200 nA during the irradiation of 0.5–2 h. The beam current was collected by the Faraday cup and was monitored on-line by using a current integrator module (Model 439, ORTEC, Oak Ridge, TN, USA) connected to a multi-channel scaler (MCS) (Model LN-6400, Laboratory Equipment Corporation, Ibaraki, Japan) which was controlled by a personal computer using Standard MAC software (Laboratory Equipment Corporation). The MCS data were recorded to calibrate beam fluctuations. The energy loss of the bombarding $^7Li^{3+}$ beams in the targets and the aluminum was taken into account using SRIM code [14, 15]. The calculated energies at the targets 29–57 MeV are listed in Table 1. Errors of the energy represent energy loss of ^{7}Li beams in the lead targets. The 51.7, 54.3 and 56.9 MeV beam energies on the targets were obtained by the bombardment with ^{7}Li particles accelerated at 60 MeV. To adjust beam energies on the targets for 45.5, 40.7, 35.3 and 28.9 MeV, an aluminum sheet of 5.4 mg/cm^2 was placed at beam upstream of the set of the lead targets. A stack of three lead targets with the corresponding Al backing and cover was used for the 60 MeV beams and two stacks of five lead targets with the Al backing and cover were used for the 50 MeV. The struggling of the beams is estimated to be less than 1.2 MeV [14, 15] which is slightly large compared with the energy loss in the lead target.

Gamma-ray spectrometry

The measurements of radioactive products in each lead target with the corresponding backing and cover sheets were carried out by a high purity germanium (HPGe) detector (ORTEC). The signals of the HPGe detector were processed using commercially available electronic modules, an amplifier (Model 572, ORTEC), a 12-bit analog to digital convertor (Model 4803A, Laboratory Equipment Corporation) and a multichannel analyzer (MCA) (Model LN-6400, Laboratory Equipment Corporation). Data taking was controlled by a personal computer using Standard MCA software (Laboratory Equipment Corporation).

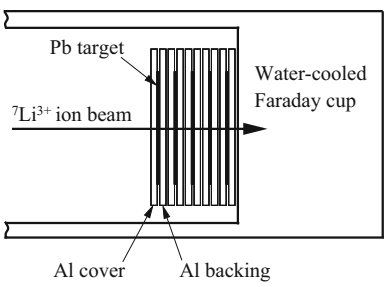

Fig. 1 Schematic view of irradiation setup

Measurement time roughly set one tenth of the time elapsed from the end of the bombardment (EOB), varying from 10 min to 8 h. The distance of samples from the cup of the detector was adjusted to be 3–30 cm. The dead time was less than 6 %. The calibration of the γ-ray spectrometry was made with a multiple gamma ray point source (Eckert & Ziegler Isotope Products) involving ^{57}Co (189 Bq), ^{60}Co (2.64 kBq), ^{88}Y (238 Bq), ^{109}Cd (271 Bq), ^{113}Sn (103 Bq), ^{137}Cs (2.32 kBq), ^{139}Ce (54 Bq) and ^{241}Am (381 Bq) with uncertainties of 2.9–3.7 % corresponding to the confidence level of 95 %. The samples were regarded as point sources because the samples had active area of approximately 5 mm in diameter which was almost identical to that of 3 mm in diameter of the multiple gamma ray point source.

A typical γ-ray spectrum for 45.5 MeV ^{7}Li + ^{nat}Pb is shown in Fig. 2. The measurement was carried out for 15 min after 2.5 h of EOB. The photopeaks of astatine isotopes $^{207-210}$At were observed. However, intense γ-rays of the astatine isotopes and those of ^{22}Na and ^{28}Mg which were produced in the reaction of ^{7}Li beam with aluminum made it impossible to measure the 687 keV photopeak ($I_\gamma = 0.26$ %) of ^{211}At by γ-ray spectroscopy. It should be noted that no photopeaks of fission fragments were observed. This shows that fission cross section is considerably small in the present reaction.

The photopeaks of $^{208-210}$At were identified not only by their photopeak energies but also by the decay curve of the counting rate of the photopeaks. Typical decay curves are shown in Fig. 3. Horizontal error bars represent the duration of the measurements. Lines show a decay curve that fits the data by using the value of the half-life reported in Ref. [16]. The errors of the fitting are 0.6, 1.0 and 1.3 % for ^{210}At, ^{209}At and ^{208}At, respectively. Nuclear data for decays of $^{207-211}$At taken from Ref. [16] are listed in Table 2.

Dry-distillation method and α-ray spectroscopy

After determining activities of $^{207-210}$At by γ-ray spectrometry, α-activities were measured by an alpha spectrometer to determine production cross sections of ^{211}At. Sources for α-spectrometry were prepared by depositing a portion of astatine solution onto a silver sheet. The astatine solution was prepared with a dry-distillation method as follows.

Table 1 Cross sections in the $^{7}Li + {}^{nat}Pb$ reactions

Energy (MeV)	^{211}At (mb)	^{210}At (mb)	^{209}At (mb)	^{208}At (mb)	^{207}At (mb)
56.9 ± 0.2	39.5 ± 2.7	290 ± 8	355 ± 9	257 ± 18	
54.3 ± 0.2	65.1 ± 6.8	431 ± 11	323 ± 8	229 ± 19	
51.7 ± 0.1	120 ± 60	471 ± 12	265 ± 7	194 ± 15	
47.7 ± 0.1	207 ± 18	353 ± 13	212 ± 8	76.0 ± 3.4	10.0 ± 1.0
45.5 ± 0.1	318 ± 25	260 ± 9	187 ± 6	32.6 ± 1.4	8.18 ± 0.76
43.0 ± 0.1	364 ± 77	201 ± 7	170 ± 6	7.24 ± 0.80	8.82 ± 0.83
40.7 ± 0.1	366 ± 40	144 ± 6	119 ± 5	2.11 ± 0.55	6.23 ± 0.54
38.0 ± 0.1	271 ± 33	117 ± 4	70.1 ± 2.7	3.77 ± 0.50	3.17 ± 0.43
35.3 ± 0.1	165 ± 19	82.8 ± 2.9	23.7 ± 0.9	3.61 ± 0.53	
32.1 ± 0.1		32.1 ± 1.2	0.67 ± 0.13	1.93 ± 0.36	
28.9 ± 0.1		3.67 ± 0.20			

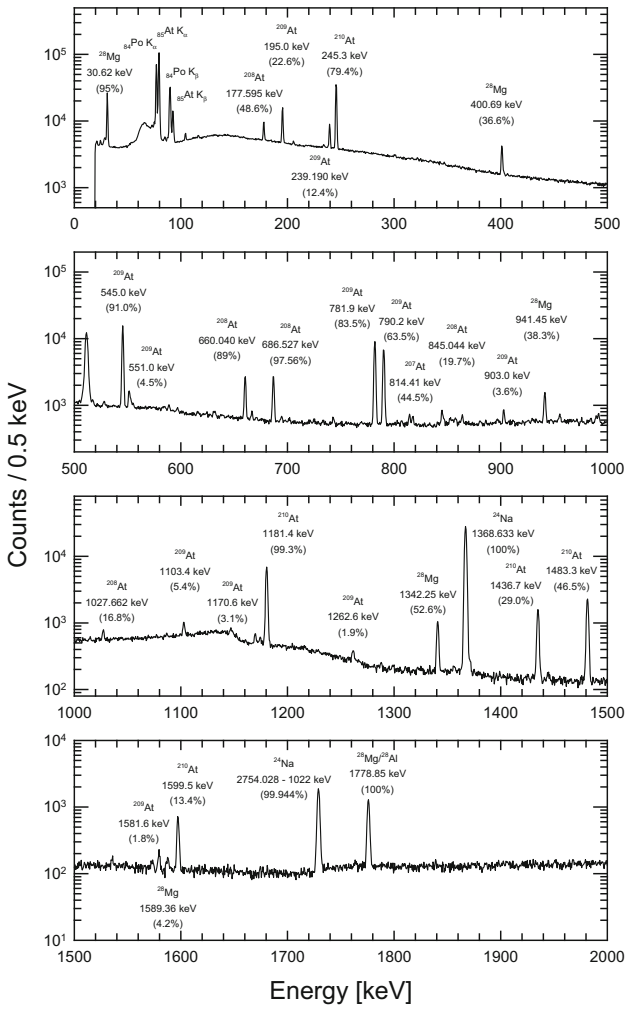

Fig. 2 Gamma-spectrum for 45.5 MeV $^{7}Li + {}^{nat}Pb$ after 2.5 h of EOB

The sample which consists of the lead target on the backing and the cover sheet was placed in a test tube of 18 cm in length and 18 mm in outer diameter. After

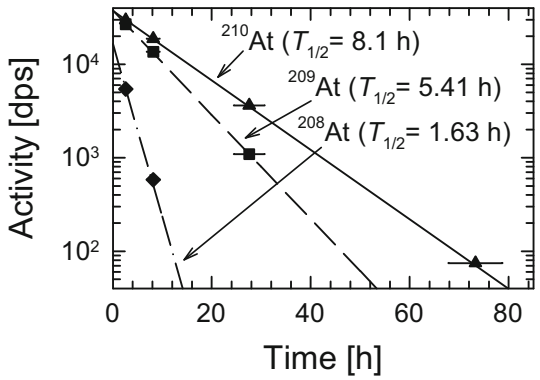

Fig. 3 Time dependence of activities of astatine isotopes ^{210}At, ^{209}At and ^{208}At

replacing air with nitrogen gas, the test tube was sealed with DuraSeal™ (Diversified Biotech, Dedham, MA, USA). A third of the portion from the bottom of the test tube was inserted into a furnace. Astatine species were distilled at 520 °C for 15–40 min. The duration of the heating was changed to study the time period to separate astatine from a melted lead target. The test tube was taken out from the furnace and was cooled down to room temperature for approximately 10 min. After opening the test tube and taking out the sample from it, the test tube was rinsed with 1.8 ml of ethanol (99.5 %, Wako Pure Chemical Industries, Ltd., Osaka, Japan), water, or diisopropyl ether (99.0 %, Wako Pure Chemical Industries, Ltd.). A portion of 5 μL from this solution including astatine was deposited on a silver sheet (99.98 %, The Nilaco Corporation, Tokyo, Japan) of 15 × 15 mm in size and 0.2 mm in thickness by a micropipette. The deposition was evaporated by a heating lamp to determine the amount of activities of $^{209-211}$At by α- and γ-ray spectrometry. No loss of the astatine in evaporation was observed in comparison with α-activities of ^{211}At measured by a liquid scintillation spectrometer PERALS (8100AB, ORDELA

Table 2 Nuclear characteristics of astatine isotopes taken from Ref. [16] and production reactions and threshold energies in the ^{7}Li + ^{nat}Pb reaction predicted by the modified HIVAP code [17]

Nuclide	Half-life	γ-ray energy (keV) (Intensity, %)	Production reaction in ^{7}Li + ^{nat}Pb[a]	Threshold energy[a] (MeV)
^{211}At	7.214 h	669.6(0.26)	^{208}Pb(^{7}Li,4n)^{211}At	30
			^{207}Pb(^{7}Li,3n)^{211}At	28
^{210}At	8.1 h	245.3(79)*, 1,181.4(99.3), 1,436.7(29.0), 1,483.3(46.5), 1,599.5(13.4)	^{208}Pb(^{7}Li,5n)^{210}At	38
			^{207}Pb(^{7}Li,4n)^{210}At	31
			^{206}Pb(^{7}Li,3n)^{210}At	28
^{209}At	5.41 h	195.0(22.6), 239.2(12.4), 545.0(91.0)*, 781.9(83.5), 790.2(63.5)	^{208}Pb(^{7}Li,6n)^{209}At	47
			^{207}Pb(^{7}Li,5n)^{209}At	38
			^{206}Pb(^{7}Li,4n)^{209}At	31
^{208}At	1.63 h	177.60(48.6), 660.04(89), 686.53(97.6)*, 845.04(19.7), 1,027.66(16.8)	^{207}Pb(^{7}Li,6n)^{208}At	48
			^{206}Pb(^{7}Li,5n)^{208}At	40
			^{204}Pb(^{7}Li,3n)^{208}At	30
^{207}At	1.80 h	588.33 (19.2)*, 814.41(44.5)	^{206}Pb(^{7}Li,6n)^{207}At	50
			^{204}Pb(^{7}Li,4n)^{207}At	33

* Photopeaks for the calculations of cross sections

[a] Predictions of the modified HIVAP code

INC.). The deposition and evaporation repeated within four times for samples with low activities. It takes 45–70 min from placement of the sample in the test tube to completion of the source for α-ray spectrometry.

Alpha particles from the source were detected by a silicon surface barrier detector (ORTEC) whose energy calibration and efficiency of 1.82 % were conducted with a standard source of 3.3 kBq (error of activity: 1 %) ^{241}Am. The confidence level of the error corresponds to 99.7 %. The alpha spectrometer was coupled to a MCA module (LN-6400, Laboratory Equipment Corporation). An α particle energy spectrum of a deposition on a silver sheet from 10 μL ethanol solution is shown in Fig. 4. The measurement was carried out for 1.7 h after 15 h of EOB. The α-decay from ^{211}At with a branching 41.8 % occurs with α-emission of 5,870 keV, while the EC decay from ^{211}At with branching of 58.2 % leads to α-emission of 7,450 keV from ^{211g}Po with a short half life of 516 ms and an α-branching 98.9 %. After α-ray spectroscopy, γ-ray spectroscopy was applied to obtain chemical yields for the preparation of the sources. Figure 5 shows a γ-ray spectrum of the alpha source corresponding to Fig. 4. The measurement was carried out for 2.0 h after 17.2 h of EOB. The chemical yield was obtained as a ratio of 245.3 keV γ-ray activities of ^{210}At before and after preparing the source. Statistical errors of the photopeak of ^{210}At (245.3 keV) in the measurements of the alpha sources cause relatively large errors of cross sections of ^{211}At. As background are present the photopeaks of ^{134}Cs (604.7 and 795.8 keV) and ^{137}Cs (661.7 keV), coming from the fallout of the accident of Fukushima Daiichi Nuclear Plant.

After distillation, the γ-activities of the lead target on the backing, the cover sheet, and the seal were measured to

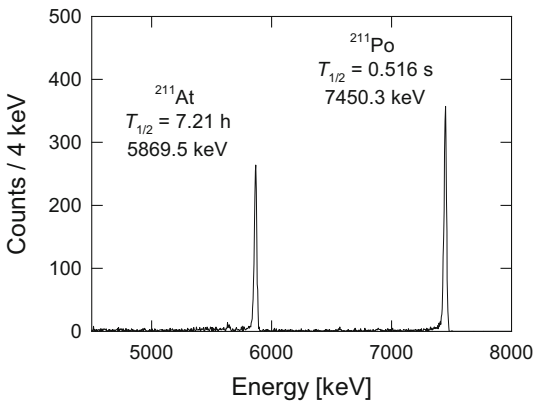

Fig. 4 Alpha-spectrum for 38.0 MeV ^{7}Li + ^{nat}Pb after 15 h of EOB

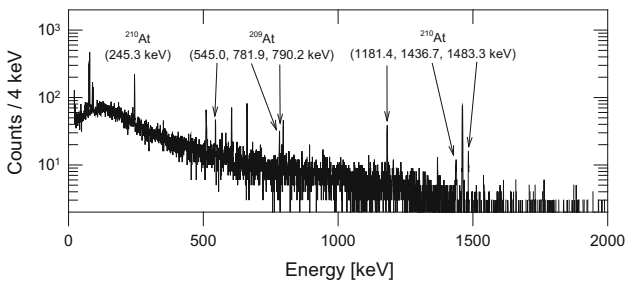

Fig. 5 Gamma-spectrum of a sample prepared for alpha spectroscopy in the 38.0 MeV ^{7}Li + ^{nat}Pb reaction after 17.2 h of EOB

determine efficiency of distillation and the distribution of activities in the test tube.

Results and discussion

Excitation functions of astatine isotopes

The excitation functions of $^{207-211}$At isotopes in the ^{7}Li + ^{nat}Pb (^{204}Pb 1.4 %, ^{206}Pb 24.1 %, ^{207}Pb 22.1 %, ^{208}Pb 52.4 %) reaction are shown in Fig. 6. The production cross section of At, σ, was calculated by the following equation,

$$\sigma = C \Big/ \left[\varepsilon_c \varepsilon I N \int_{t0-T}^{t0} \varphi(t) e^{-\lambda t} \delta t \right], \quad (1)$$

where C is the counting rate of the photopeak or α peak at the end of irradiation $t0$, ε_c the chemical yield, ε the detection efficiency of photopeak or α-particle, I the emission probability of γ-ray or α-particle, N the number of ^{nat}Pb target atoms, $\varphi(t)$ the beam flux, λ the decay constant and T the irradiation time. The beam flux (t) recorded by the MCS was used to be considered the change of the beam flux as a function of irradiation time.

Lines show the cross sections of $^{207-211}$At isotopes calculated by the modified HIVAP code [17] in which the statistical model code HIVAP [18] is coupled with the CCDEF code [19]. A statistical model calculation by the modified HIVAP was independently carried out with the input parameters which systematically well reproduced a large number of experimental fusion–evaporation cross sections in the similar heavy ion reactions without adjusting the input parameters to fit the present experimental data. It should be noted that calculations rather well reproduce experimental data. Large deviations of experimental data point at 29 MeV could be due to uncertainty of the statistical calculation.

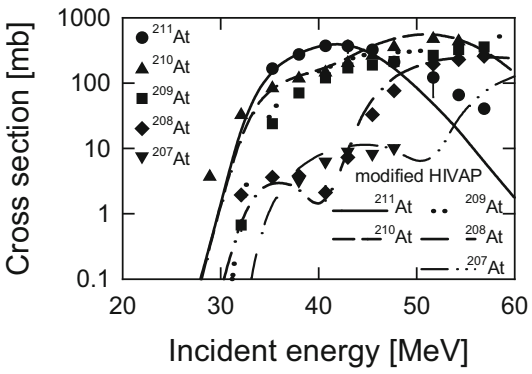

Fig. 6 Excitation functions of $^{207-211}$At isotopes in the ^{7}Li + ^{nat}Pb reaction

From the comparison of experimental data with the statistical calculation, information on nuclear reaction can be obtained. Production reactions of each astatine isotope in the ^{7}Li + ^{nat}Pb reaction and their threshold energies predicted by the modified HIVAP code [17] are listed in Table 2. Figure 7 shows excitation functions of each astatine isotopes, indicating contributions of reaction channels in the ^{7}Li + ^{nat}Pb reaction. The calculated excitation functions (lines) are represented by weighted values with natural atom percent abundance of lead isotopes (^{204}Pb 1.4 %, ^{206}Pb 24.1 %, ^{207}Pb 22.1 %, ^{208}Pb 52.4 %,). Total cross sections shown by solid symbols and thick lines in Fig. 7 correspond to those in Fig. 6. For comparison, experimental data points reported in Ref. [13] are plotted by open symbols. Some points show large deviation from the present data.

As shown in Figs. 6 and 7a, ^{211}At which is a prospected candidate for targeted alpha therapy yields the maximum approximately 390 mb at 41 MeV mainly through the ^{208}Pb(^{7}Li,4n)^{211}At reaction. The maximum cross section of this reaction is about half of 800 mb at 28 MeV in ^{209}Bi(α,2n)^{211}At reaction [1–7]. ^{207}Pb(^{7}Li,3n)^{211}At reaction slightly contributes production at the energy region close to fusion barrier.

As shown in Figs. 6 and 7b, ^{210}At was produced via ^{206}Pb(^{7}Li,3n)^{210}At, ^{207}Pb(^{7}Li,4n)^{210}At and ^{208}Pb(^{7}Li,5n)^{210}At reactions in this energy range. Although the cross section of ^{210}At becomes smaller than those of ^{211}At below 44 MeV, ratios of the cross section of ^{210}At to that of ^{211}At are larger than 0.4. ^{210}At ($T_{1/2}$ = 8.1 h) decays with EC-branching of 99.8 %, leading to the long lived α-emitter of ^{210}Po ($T_{1/2}$ = 138 days). It is well known that ^{210}Pb has high radiotoxicity characterized as its decay mode and behavior in the human body tissue. Therefore, the astatine tracer produced through ^{7}Li + ^{nat}Pb could not be adapted to clinical uses but useful to fundamental researches. Because of high-energy γ-rays of ^{210}At it is easy to detect At and trace At compounds in chemical process without making a source for α-ray spectrometry.

The nuclide ^{209}At was produced through ^{206}Pb(^{7}Li,4n)^{209}At, ^{207}Pb(^{7}Li,5n)^{209}At, and ^{208}Pb(^{7}Li,6n)^{209}At reactions which correspond to the neutron evaporation channels with one more neutron of the production of ^{210}At. This results in high threshold energy at 31 MeV and large predicted cross sections above 56 MeV compared with those of ^{210}At. ^{209}At ($T_{1/2}$ = 5.41 h) decays with EC-branching of 95.9 %, leading to the long lived α-emitter of ^{209}Po ($T_{1/2}$ = 102 y), and with α-branching of 4.1 %, leading to the EC-decaying radioisotope ^{205}Bi ($T_{1/2}$ = 15.3 days). Activities of daughters ^{209}Po and ^{205}Bi are negligibly smaller than that of the parent ^{209}At due to their long life and small branching, respectively. A high-energy emitter (545, 782, 790 keV) ^{209}At could be a useful astatine tracer for fundamental researches as well as ^{210}At.

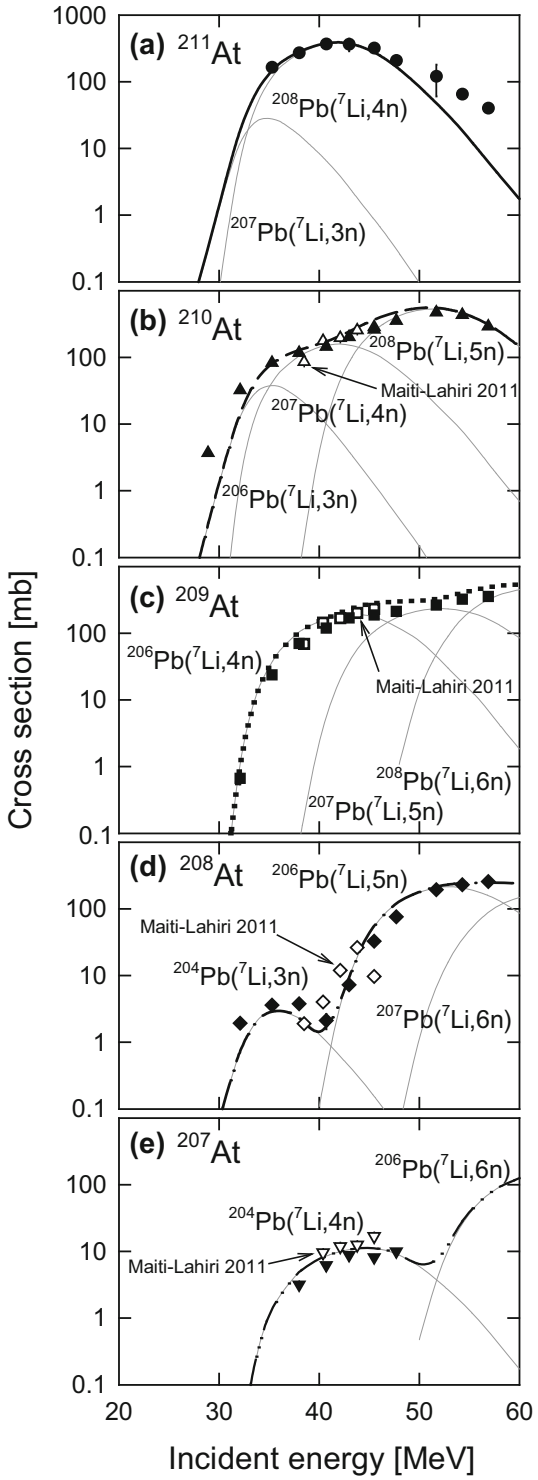

Fig. 7 Excitation functions of At isotopes in the $^{7}Li + {}^{nat}Pb$ reaction: **a** ^{211}At, **b** ^{210}At, **c** ^{209}At, **d** ^{208}At and **e** ^{207}At

The nuclides ^{208}At and ^{207}At were produced through $^{204}Pb(^{7}Li,3n)^{208}At$, $^{206}Pb(^{7}Li,5n)^{208}At$ and $^{207}Pb(^{7}Li,6n)^{208}At$ reactions, and $^{204}Pb(^{7}Li,4n)^{207}At$ and $^{206}Pb(^{7}Li,6n)^{207}At$ reactions, respectively. The absence of ^{205}Pb in atomic percent abundance provides dips in total cross sections at 40 MeV for ^{208}At and at 50 MeV for ^{209}At. ^{208}At ($T_{1/2} = 1.63$ h) decays with EC-branching of 99.5 %, leading to the long lived α-emitter of ^{208}Po ($T_{1/2} = 2.90$ years). ^{207}At ($T_{1/2} = 1.80$ h) decays with EC-branching of 91.4 %, leading to the EC-decaying radioisotopes ^{207}Po ($T_{1/2} = 5.8$ h)–^{207}Bi ($T_{1/2} = 31.6$ years). Activities of these daughters are negligibly small compared with their parents. Lack of present data of ^{207}At at incident energies higher than 50 MeV is due to long cooling time 11 h before starting γ-ray measurements.

Finally, it should be noted that the effect of break up reaction of ^{7}Li appears at higher incident energies as shown in Fig. 8 in which excitation functions are indicated in a linear scale. The trend of measured cross sections in this work is well represented by the predictions of the modified HIVAP in the logarithm plots of Figs. 6 and 7. In Fig. 8, however, slightly larger deviations, namely, small experimental cross sections of ^{210}At and ^{209}At compared with the calculations are clearly observed at incident energies higher than 44 MeV. This suppression of the experimental cross sections is considerably large because the cross sections correspond to main channels in complete fusion at energies higher than 44 MeV. The suppression probably originates from the effect of breakup reaction of ^{7}Li as discussed in Ref [9, 10]. The breakup reaction is not taken into consideration in the modified HIVAP code [17]. In general, the statistical model calculations including HIVAP [17, 18] and JOANNE2 [9, 10] calculate only complete fusion cross sections. The missing complete fusion cross sections observed as suppression are found in yields of incomplete fusion including breakup reaction.

Dry-distillation of astatine isotopes

From the measurements of activities of astatine isotopes after distillation, it is found that yields increase with the duration of heating and become almost constant over 20 min. A large portion of approximately 85 % of astatine

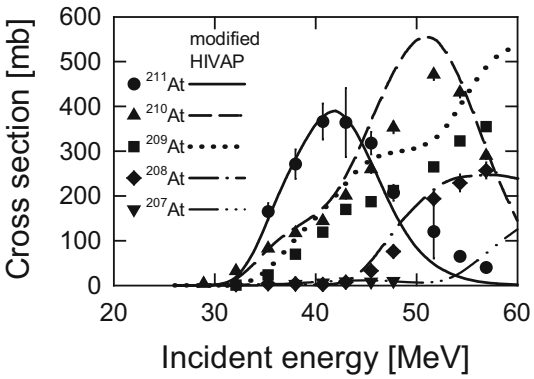

Fig. 8 Excitation functions of $^{207-211}At$ isotopes in a linear scale

products were found to be released from the lead target on the aluminum backing sheet but about 15 % of products were not released. Because the astatine isotopes produced in lead near the aluminum backing sheet at the beam-forward side within approximately 160 μg/cm^2 from the boundary between lead and aluminum were implanted into the aluminum backing sheet owning to recoil energy of approximately 1.4 MeV brought into the compound nuclei by the incident ^{7}Li. Such 15 % astatine products implanted into the aluminum were not released from the aluminum by heating 520 °C, while 85 % astatine products were released from the melted lead and then attached on the inner wall of the test tube (80 %) and on the seal (5 %). The seal was disposed to prevent from contamination. Therefore, approximately 80 % of astatine isotopes produced by irradiation can be used. Increasing of lead target in thickness results in decrease of fraction of the astatine implanted into aluminum.

No-carrier-added astatine was obtained by rinsing the test tube with solutions of 1.8 mL. Overall recovery yields of astatine were approximately 65 % for ethanol and water; 25 % for diisopropyl ether. Ethanol and water easily removed a large portion of approximately 80 % of astatine from the inner wall of the test tube but diisopropyl ether did only 30 %. The difference of recovery yields between the solutions could involve information on chemical forms of astatine attached on the inner wall of the test tube by dry-distillation. Although the recovery yields depend on solutions, any aqueous and organic solution involving astatine could be easily prepared by this chemical separation procedure, namely, dry-distillation and following rinsing.

Conclusions

Excitation functions of astatine isotopes $^{207-211}$At in the 29–57 MeV ^{7}Li + ^{nat}Pb reaction were determined and were compared with the predictions of the statistical calculation using the modified HIVAP code. The α-emitting nuclide ^{211}At ($T_{1/2}$ = 7.2 h) is mainly produced through ^{208}Pb(^{7}Li,4n)^{211}At with maximum cross section of 390 mb at 41 MeV. The γ-emitting nuclides ^{210}At ($T_{1/2}$ = 8.1 h) and ^{209}At ($T_{1/2}$ = 5.41 h) have large cross sections at higher incident energies compared with ^{211}At. The results show that the ^{7}Li + ^{nat}Pb reaction provides a production route of astatine isotopes not for clinical uses but for fundamental research. The effects of breakup reaction of ^{7}Li probably result in the suppression of complete fusion reaction at energy higher than 44 MeV.

We developed a chemical procedure based on dry-distillation which easily separates astatine isotopes from an irradiated lead target with high radiochemical and chemical purity, and high yield.

Astatine tracer solution produced with this procedure would make one able to study chemical forms of astatine in the tracer solution, the synthesis of amino acid derivatives labeled with astatine, and so on.

Acknowledgments The authors thank the crew of the JAEA Tandem Accelerator for the accelerator operation. We are thankful to M. Asai for his help for γ-ray and α-ray spectroscopies. This work was supported by JSPS KAKENHI Grant Number 2360013.

References

1. Lambrecht RM, Mirzadeh S (1985) Int J Appl Radiat Isot 36:443–450
2. Larsen RH, Wieland BW, Zalutsky MR (1996) Appl Radiat Isot 47:135–143
3. Henriksen G, Messelt S, Olsen E, Larsen RH (2001) Appl Radiat Isot 54:839–844
4. Hermanne A, Tárkányi F, Takács S, Szücs Z, Shubin YN, Dityuk AI (2005) Appl Radiat Isot 63:1–9
5. Lebeda O, Jiran R, Ráliš J, Štursa J (2005) Appl Radiat Isot 63:49–53
6. Groppi F, Bonardi ML, Birattari C, Menapace E, Abbas K, Holzwarth U, Alfarano A, Morzenti S, Zona C, Alfassi ZB (2005) Appl Radiat Isot 63:621–631
7. Morzenti S, Bonardi ML, Groppi F, Zona C, Persocp E, Menapace E, Alfassi ZB (2008) J Radioanal Nucl Chem 276:843–847
8. Freiesleven H, Britt HC, Birkelund J, Huizenga JR (1974) Phys Rev C 10:245–249
9. Dasgupta M, Hinde DJ, Hagino K, Moraes SB, Gomes PRS, Anjos RM, Butt RD, Berriman AC, Carlin N, Morton CR, Newton JO, Toledo AS (2002) Phys Rev C 66:04602-1-4
10. Dasgupta M, Gomes PRS, Hinde DJ, Moraes SB, Anjos RM, Berriman AC, Butt RD, Carlin N, Lubian J, Morton CR, Newton JO, Toledo AS (2004) Phys Rev C 70:024606-1-20
11. Penionzhkevich YE, Lukyanov SM, Astabatyan RA, Demekhina NA, Ivanov MP, Kalpakchieva R, Kulko AA, Markaryan ER, Maslov VA, Muzychaka YA, Revenko RV, Skobelev NK, Smirnov VI, Sobolev YG (2009) J Phys G 36:025104-1-12
12. Roy K, Lahiri S (2008) Appl Radiat Isot 55:571–576
13. Maiti M, Lahiri S (2011) Phys Rev C 84:067601-1-4
14. Ziegler JF (1985) The stopping and range of ions in solids. Pergamon Press, New York
15. Ziegler JF, Biersack JP (2013) SRIM-2013 Code, http://www.srim.org
16. Firestone RB (1996) Table of Isotopes, 8th edn. Wiley, New York
17. Nishio K, Ikezoe H, Mitsuoka S, Lu J (2000) Phys Rev C 62:014602-1-12
18. Reisdorf W, Schädel M (1992) Z Phys A 343:47–57
19. Fernandez-Niello J, Dasso CH, Landowne S (1989) Comput Phys Commun 54:409–412